

Improving functional properties of Spirulina protein by covalent conjugation followed by complex coacervation processes

Zijia Zhang^{a,*}, Bo Wang^b, Greg Holden^c, Jie Chen^d, Benu Adhikari^{a,e,*}

^a School of Science, RMIT University, Melbourne, VIC 3083, Australia

^b School of Behavioural and Health Science, Australian Catholic University, Sydney, NSW 2060, Australia

^c Bega Corporate Centre, Melbourne, VIC 3008, Australia

^d State Key Laboratory of Food Science and Technology, Jiangnan University, Wuxi, China

^e Centre for Advanced Materials and Industrial Chemistry (CAMIC), RMIT University, Melbourne, VIC 3001, Australia

ARTICLE INFO

Keywords:

Spirulina protein concentrate
Maltodextrin
Carrageenan
Maillard reaction
Complex coacervation
Microencapsulation

ABSTRACT

Two stage complexation processes, i.e., covalent conjugation followed by complex coacervation processes were used to improve functional properties of *Spirulina* protein. Conjugates of *Spirulina* protein concentrate (SPC)-maltodextrin (MD) were produced via wet-route Maillard reaction and they were coacervated with carrageenan (CG). The complex coacervates of mixture of unconjugated SPC and MD with CG was used as benchmark. (SPC-MD conjugate)-CG coacervate and (SPC-MD mixture)-CG coacervate were used as shell material to encapsulate oxidation sensitive canola oil. The optimum conditions for the complex coacervation were found at pH 3.0 and ratio of conjugate- or mixture-to-CG ratio of 24:1 (w/w). Spray-dried microcapsules of canola oil produced using (SPC-MD conjugate)-CG coacervates exhibited lower surface oil content (1.52%), higher encapsulation efficiency (92.5%), and smaller particle size ($D_{50}=7.66\ \mu\text{m}$) compared to those produced using mixture-based coacervates as shell materials. The microcapsules produced using conjugate-based coacervates as shell material showed improved oxidative stability. These findings suggests that the Maillard reaction induced conjugate of SPC and its complex coacervates can be promising encapsulating shell materials for oxidation sensitive oils.

1. Introduction

Edible oils are important part of human diet, and they are also widely used as food ingredients by food industry. In recent years, oils with high polyunsaturated fatty acids (PUFAs) content such as tuna, flaxseed and canola oils are increasingly becoming popular among consumers because of their health benefits including protection against inflammation (Oppedisano et al., 2020), cardiovascular diseases (Ganesan et al., 2018) and cancers (Eltweri et al., 2017). However, these bioactive oils can readily undergo oxidation during food processing and storage, which compromises the nutritional value and acceptability of the food product (Pham et al., 2020). To tackle this issue, microencapsulation technology has been used by food industry to stabilise PUFAs-rich oils in a protective shell to extend shelf-life.

To date, oils can be encapsulated by a number of technologies including spray drying, freeze drying, coacervation, emulsification and fluidised bed coating etc. (Đorđević et al., 2015; Ray et al., 2016). Among these technologies, complex coacervation followed by spray

drying is one of the most effective methods to protect the PUFAs enriched oils against oxidation (Lan et al., 2021). Complex coacervation is a liquid-liquid phase separation where a polymer-rich phase separates from the aqueous phase. The polymer-rich phase is formed through electrostatic interaction between two oppositely charged polymers. Proteins and polysaccharides are commonly used as oppositely charged food molecules in this process (Schmitt and Turgeon, 2011). Protein-polysaccharide complex coacervates exhibit surface-active nature of protein and gel structure-forming capacity of polysaccharides and also show enhanced steric hindrance effect against undesired interactions. This ultimately improves the protection of the encapsulated PUFAs-rich oils. The complex coacervation process has the superiority in producing microcapsules with compact structures, high oil loading (up to 60%, w/w), low surface oil content, as well as improved control-released properties (Wang et al., 2014).

Although a number of studies were undertaken to develop protein-polysaccharide complex coacervates as encapsulants to encapsulate PUFAs-rich oils (Lan et al., 2021; Pham et al., 2020), the study of com-

* Corresponding author at: School of Science, RMIT University, Melbourne, VIC 3083, Australia.

** Corresponding author.

E-mail addresses: s3714749@student.rmit.edu.au (Z. Zhang), benu.adhikari@rmit.edu.au (B. Adhikari).

plex coacervation process using protein-polysaccharide conjugates (produced via Maillard reaction) and commonly available polysaccharides has been rarely reported. The development of this novel delivery system and the characterization of the resulting microcapsule would be interesting from fundamental as well as application perspective. This is because Maillard reaction products (MRPs) are known to be effective in stabilising bioactive oils (Ifeduba and Akoh, 2016). Previous work has shown that the solubility and emulsifying properties of proteins can be significantly improved by conjugating with carbohydrates and the application of resulting conjugates produces substantially stable oil-in-water emulsions (Martinez-Alvarenga et al., 2014). Muhoza et al. (2022) produced gelatin-low methoxyl pectin conjugate using wet-heating route, and the complex coacervates were produced by these conjugates to encapsulate cinnamaldehyde. This work showed the enhanced encapsulation efficiency and stability to ionic strength of microcapsules compared to those produced using unconjugated protein-carbohydrate coacervates (Muhoza et al., 2022). Stearidonic acid soybean oil was encapsulated using coacervates of Maillard reaction modified gelatin and gum Arabic (Ifeduba and Akoh; 2016) and the results showed that the oxidative stability of the resulting microcapsules using this system was substantially higher compared to when Maillard reaction-induced conjugation was not carried out before the complex coacervation. This improved oxidative stability of the emulsions and microcapsules was attributed to the antioxidative property of protein-carbohydrate conjugates. Therefore, it is of practical importance to further study the effectiveness of conjugated protein (through Maillard reaction) as an emulsifier and encapsulant in the microencapsulation of oil through complex coacervation.

Many biopolymeric materials such as whey protein, soy protein, gelatin, gum Arabic and alginate are commonly used in the microencapsulation process due to their desirable rheological, emulsifying and encapsulating properties (Kaushik et al., 2015; Rudke et al., 2019). Algal proteins are emerging as important alternative proteins with promising application in food industry (Onwezen et al., 2021; Rawiwan et al., 2022). However, there is still a paucity in research on their investigating as encapsulating materials of bioactive compounds. It was reported that *Spirulina* microalgae protein showed promising nutritional property and its emulsifying and encapsulating properties was significantly improved via the Maillard reaction (Zheng et al., 2020). In our earlier work, the Maillard reaction-based conjugation process of *Spirulina* protein and maltodextrin was studied and the resulting conjugates were characterised (Zhang et al., 2023).

In the above context, this work aimed to take the research on *Spirulina* protein and its conjugate further and study the complex coacervation process of *Spirulina* protein-maltodextrin conjugates with commonly available polysaccharide and quantify the efficacy of these conjugate-based coacervates to protect PUFAs-rich oils.

2. Materials and methods

2.1. Materials

Spirulina powder (Bioglan Pty Ltd., New South Wales, Australia) was purchased from a local Chemist Warehouse outlet (Melbourne, Australia). Maltodextrin (MD) (GLUCIDEX® 39) and λ -carrageenan (CG) (GENUVISCO® CSW-2, Lambda) were kindly provided by Roquette Pty Ltd. (Lestrem, France). Canola oil was purchased from the local market. Transglutaminase (TG) Sprinkle Powder (Activa KS-LS) was purchased from Melbourne Food Depot (Melbourne, Australia). Chemicals used in this study including hydrochloric acid, sodium hydroxide, glacial acetic acid, n-hexane, isopropanol, methanol, 1-butanol anhydrous, barium chloride, ammonium thiocyanate, 2,2,4-Trimethylpentane (isooctane), anhydrous ferric chloride, ferrous sulfate and *p*-Anisidine were of analytical grade and were purchased from Sigma-Aldrich Pty Ltd. (New South Wales, Australia).

2.2. Extraction of *Spirulina* protein

A schematic diagram illustrating all experimental steps involved in this study is presented in Fig. 1. The *Spirulina* protein concentrate (SPC) was extracted according to the procedure reported previously (Zhang et al., 2023). In brief, *Spirulina* powder was mixed with Milli Q water (powder-to-water ratio: 1:15, w/w), the mixture was then adjusted to pH 10.0 using 1 M NaOH. The suspension was agitated at 800 rpm and room temperature for 2 h and then centrifuged at 9000 × g and 4 °C for 30 min to obtain the supernatant. The supernatant was collected and its pH was adjusted to 3.5 using 1 M HCl. The precipitated protein was recovered by centrifuging the mixture at 9000 × g and 4 °C for 30 min. Milli Q water was added to the protein precipitate at a precipitate-to-water ratio of 1:30 (w/w) and the mixture was adjusted to pH 7.0. Finally, these extracted proteins were freeze dried at 10 Pa and –80 °C for 48 h (VaCo 10, ZIRBUS technology GmbH, Harz, Germany). The extracted SPC contained 78.9 ± 0.9% protein, 1.9 ± 0.6% lipid and 3.9 ± 0.1% moisture, measured by using Kjeldahl method, AOAC Method No. 920.85, and AOAC Method No. 925.10, respectively. The SPC powder was vacuum sealed and stored at 4 °C before use.

2.3. Preparation of SPC-MD conjugates

SPC-MD conjugates were prepared according to the process reported previously (Zhang et al., 2023). Briefly, SPC-MD mixture (1:1, w/w) was dispersed in Milli Q water at a polymer-to-water ratio of 1:9 (w/w). The dispersion was agitated at 300 rpm and 4 °C for 2 h and then its pH was adjusted to 10.0 using 1 M NaOH, followed by agitation at 4 °C overnight. Subsequently, the solution was incubated at 60 °C for 6 h using a preheated shaking bath to induce the SPC-MD conjugation through wet-heating route. The samples were collected after 6 h heating, and immediately cooled in an ice bath to stop the reaction. The resulting solution was neutralised using 1 M HCl and dialysed using a dialysis bag (cut-off molecular weight of 3–5 kDa) (Thermo Fisher Scientific, New South Wales, Australia) for 10 h to remove the unreacted MD. The dialysed SPC-MD conjugates were finally freeze-dried at 10 Pa and –80 °C for 48 h. This SPC-MD conjugate powder was vacuum sealed and stored at 4 °C before use.

2.4. Optimization Of Complex Coacervation Process

2.4.1. Preparation of SPC-MD mixture and conjugate and CG stock solutions

SPC-MD mixture, SPC-MD conjugate and CG stock solutions were prepared separately at a total polymer concentration of 0.3% (w/w). Briefly, the SPC-MD mixture (with a SPC:MD ratio of 1:1, w/w), SPC-MD conjugate and CG were dissolved in the Milli Q water and the mixtures were agitated at 300 rpm for 2 h. These stock solutions were adjusted to pH 7.0 and stored at 4 °C before use.

The effects of pH and polymer ratio (SPC-MD mixture- or conjugate-to-CG ratio, w/w) on complex coacervation were studied and optimised. Briefly, the above stock solutions were mixed at different ratios and the mixed solutions were adjusted to pH 2.0–7.0 using 0.5 M HCl solution to induce the complex coacervation. The optical density and the zeta-potential values of complex coacervates were measured after stabilizing at room temperature for 2 h.

2.4.2. Measurement of optical density

The optical density of the dispersions of complex coacervates was measured as a function of pH and mixing ratio. The SPC-MD mixture or conjugate solution was mixed with CG solution, at a mixture- or conjugate-to-CG ratio of 6:1, 12:1, 24:1 and 36:1 (w/w), respectively. The total polymer content of solution was controlled at 0.3% (w/w). These mixed solutions were adjusted to pH 2.0–3.5 using 0.5 M HCl with an increment of 0.25 and their light absorption at 400 nm was

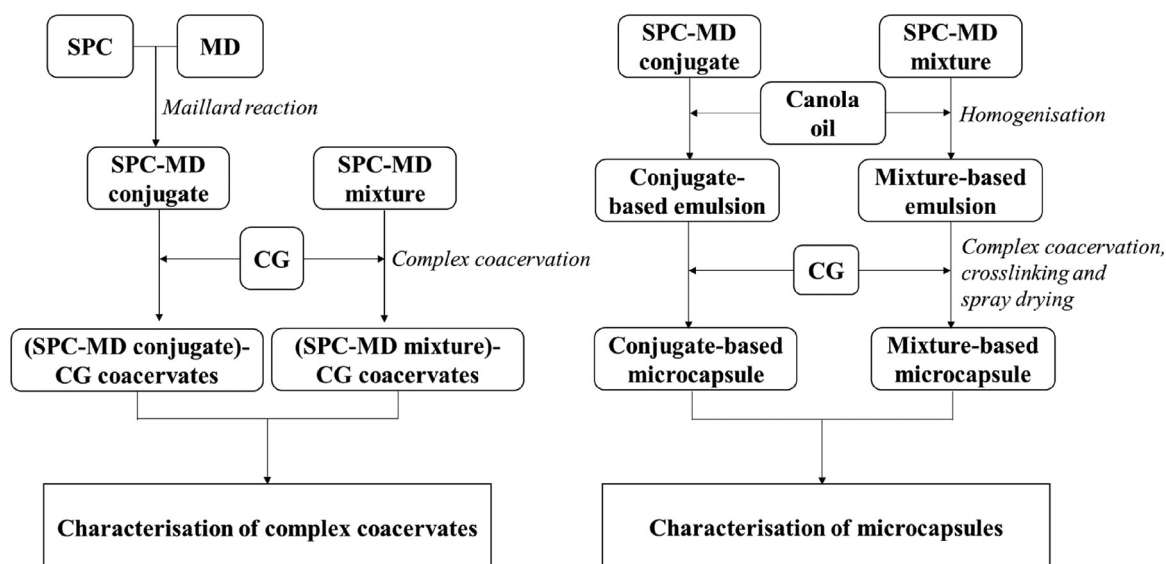


Fig. 1. Full schematic representation of experimental plan to optimize complex coacervation between SPC-MD mixture or conjugate and CG, and the encapsulation of canola oil using the (SPC-MD mixture)- or (SPC-MD conjugate)-CG coacervates as wall materials. SPC: Spirulina protein concentrate; MD: maltodextrin; CG: carrageenan.

determined using a UV spectrophotometer (Lambda 35, PerkinElmer., USA).

2.4.3. Measurement of zeta-potential

The solutions of MD, CG, SPC-MD mixture, SPC-MD conjugate, SPC-MD mixture-CG and SPC-MD conjugate-CG were prepared by dissolving these polymers in the Milli Q water at a total polymer content of 0.3% (w/w). The ratio of the SPC-MD mixture or conjugate and CG was controlled at 24:1 (w/w) based on data obtained in Section 2.4.2. These solutions were then adjusted in the pH range of 2.0–7.0 using 0.5 M HCl or NaOH and their zeta-potential values were measured using a zeta sizer (Nano-ZS, Malvern Instruments Ltd., Malvern, UK).

2.4.4. Rheological measurements

The (SPC-MD mixture)-CG and (SPC-MD conjugate)-CG solutions with a total polymer content of 3.0% (w/w) were prepared. Storage (G') and loss (G'') moduli of the complex coacervates at different mixture- or conjugate-to-CG ratios and pH values were measured using a rheometer (Discovery HR-1, TA Instruments Ltd., USA). A stainless-steel parallel plate (40 mm) with a 1 mm gap between flat surfaces was used. Before each measurement, the coacervate samples were loaded and equilibrated at 25 °C for 2 min. The apparent viscosities of the dispersions were measured in the shear rate range of 0.01–120 s^{-1} at 25 °C. The oscillation frequency sweep tests over 0.05–10 Hz were performed at 25 °C, with a strain amplitude of 1%. This amplitude was within the linear viscoelastic region, determined by the preliminary strain sweeps experiments.

2.5. Microencapsulation of canola oil

Briefly, 250 g SPC-MD mixture and conjugate solutions (6% w/w) and CG dispersions (0.25%, w/w) were prepared by dissolving SPC-MD mixture (SPC:MD ratio: 1:1, w/w), conjugates and CG separately in the Milli Q water with the agitation at 600 rpm and 40 °C for 2 h. Canola oil (5.21 g) was added to SPC-MD mixture or conjugate solution and it was homogenised using a Ultra-Turrax homogenizer at 12,000 rpm for 5 min to obtain a coarse oil-in-water emulsion. This O/W emulsion was subsequently homogenised at 60 MPa using a microfluidiser (M-110 L, Microfluidics, Newton, MA) for 3 passes to produce fine emulsion. Then, the CG dispersion (0.25%, w/w) was slowly added into the emulsion and the mixture was agitated at 800 rpm and 40 °C. In all the formulations,

the total polymer content of the mixture was 25% (w/w), with a core-to-wall ratio of 1:3 (w/w). The pH of the mixed emulsion was then adjusted to pH 3.0 using 1 M HCl to induce complex coacervation, and it was cooled down to 5 °C to facilitate the formation of liquid microcapsules. The temperature of the coacervates was controlled at 5 °C for 30 min and 50 mL 2% (w/w) transglutaminase solution was added. The liquid microcapsules were agitated at 800 rpm and at room temperature for 5 h to complete crosslinking. These liquid microcapsules were then spray dried to produce microcapsule powder.

2.6. Spray drying

The liquid microcapsules formed in Section 2.5 were spray dried using a laboratory-scale Mini Spray Dryer (Büchi Corporation, New Castle, DE, USA) equipped with a twin-fluid atomizing nozzle ($d = 0.5$ mm diameter). The inlet temperature and the flow rate of the feed were controlled at 170 °C and 8 mL/min, respectively to maintain the outlet temperature of 90 ± 2 °C. This spray-dried solid microcapsule powder was stored at 4 °C until further use.

2.7. Physicochemical properties of microcapsules

2.7.1. Moisture content and water activity

The moisture content and water activity (a_w) of spray-dried microcapsules were determined using a moisture analyser balance (MB45 Ohaus, Parsippany, NJ, USA) and a water activity meter (Aqualab CX-2, Pullman, WA, USA), respectively.

2.7.2. Encapsulation efficiency

The surface oil content of powder microcapsule samples was measured according to Wang et al. (2014)'s method with a minor modification. Briefly, 2.0 g of microcapsule powder was mixed with 30 mL of hexane and vortexed for 60 s. After centrifugation at $6000 \times g$ and 20 °C for 15 min, the supernatant was filtered into a pre-weighed tube using filter paper (Whatman No.1). Then, the filtrate was stored in a fume hood for 12 h to allow the evaporation of the organic solvent. Finally, the extracted oil was heated at 80 °C for 1 h, followed by cooling to room temperature. The weight of the extracted oil was measured.

The total oil content of microcapsule was measured as Kim et al. (2005) described in their report. Briefly, 2.0 g of microcapsule powder was mixed with 8 mL Milli-Q water and vortexed for 2 min.

The dispersion was then added with 45 mL of hexane/isopropanol (3:1, v/v) mixture and stirred at 300 rpm for 30 min. The dispersion was centrifuged at $6000 \times g$ and 20°C for 15 min. The organic solvent phase (upper layer) was separated, and the oil in the lower layer was re-extracted using the same amount of solvent, followed by centrifugation. Then all the separated organic solvent phase were combined, filtered and stored in the fume hood for 12 h and heated at 80°C for 1 h. The weight of the oil was measured. The encapsulation efficiency (EE,%) was calculated using Eq. (1).

$$EE (\%) = \frac{W_{to} - W_{so}}{W_{to}} \times 100 \quad (1)$$

Where, W_{to} (g) and W_{so} (g) are the total oil weight and surface oil weight of microcapsule, respectively.

2.7.3. Particle size of microcapsules

The particle size (D_{50}) of the microcapsules was measured using a Mastersizer (Malvern Instruments Ltd., Malvern, UK). The microcapsules were dispersed in Milli Q water and agitated at 300 rpm for 10 min. Then the dispersion was transferred to the particle size analyser for the measurement. The refractive index the particle and dispersant were set at 1.52 and 1.33, respectively.

2.7.4. Denaturation temperature

The thermal characteristics of the microcapsule samples were analysed using differential scanning calorimetry (DSC Q-2000, TA Instruments, New Castle, DE, USA). Briefly, 5 mg of microcapsule powder solution was weighed in an aluminum pan and sealed, and an empty sealed pan was used as reference. Samples were heated from 20 to 150°C at a heating rate of $10^\circ\text{C}/\text{min}$ under nitrogen gas flush at 20 mL/min purge rate. The denaturation temperature (T_d) and the enthalpy variation were analysed via UniversalTM software (TA Instruments, New Castle, DE, USA).

2.7.5. FTIR analysis of microcapsules

The FTIR spectra of SPC, MD, CG, SPC-MD conjugate, microcapsules produced by (SPC-MD mixture)-CG and (SPC-MD conjugate)-CG coacervates were analysed using a FTIR spectrometer (Perkin Elmer, CT, USA). All the spectra of the test samples were average of 64 scans from 4000 to 400 cm^{-1} at a resolution of 1 cm^{-1} .

2.8. Morphology of microcapsules

The morphology of the microcapsule powders was obtained using a scanning electron microscope (FEI Quanta 200 ESEM, Japan). The samples were coated with palladium using a Sputter Coater (VG Microtech, England). Images were captured under magnification of $5000\times$ and an accelerating voltage of 10 kV.

2.9. Surface composition of microcapsules

Surface composition of the microcapsule powders was determined using X-ray photoelectron spectroscopic (XPS) technique according to Gaiani et al. (2010). Briefly, the microcapsule powders were placed in a sample holder and degassed in high vacuum (1.8×10^{-8} mBar) for 24 h before it was transferred to the analysis chamber. Then the sample was scanned using a K-Alpha Thermo Scientific photoelectron spectrometer (K-alpha, Thermo Fischer Scientific, USA). The general spectra were obtained and the area of C_{1s} , N_{1s} and O_{1s} was determined using the Casa XPS software (V2.3.5, Casa Software Ltd., UK). Shirley baseline and Gaussian/Lorentzian (50/50%) peaks were used for the background subtraction and spectral decomposition, respectively. The protein content on the microcapsule surface was calculated as $N \times 6.25$.

2.10. Oxidative stability of spray-dried microcapsules

Microcapsule powders were sealed in a screw-capped vial (20 mL) and stored at 40°C for 4 weeks to accelerate the oil oxidation. During the storage, the microcapsule powder was sampled out weekly and the total oil was extracted using the protocol described in Section 2.7.2. The peroxide and p-Anisidine values of the oil after storage were evaluated to determine the oil oxidative stability. Canola oil was used as the control.

2.10.1. Determination of peroxide value

The peroxide value (PV) was determined according to International Dairy Federation (IDF)'s standard method with minor modification (Shantha and Decker, 1994). Briefly, 10 mg of extracted oil was mixed with 3 mL of the methanol-butanol mixture (2:1, v/v). Ammonium thiocyanate solution (15 μL , 3.94 M) and ferrous chloride solution (15 μL , 0.072 M) were then added to the samples and vortexed for 30 s. The sample was placed in the dark for 20 min and the absorbance of each solution at 510 nm was measured using a microplate reader. The PV of the oil was calculated using Eq. (2) and expressed as milliequivalents of O_2/kg oil.

$$PV = \frac{(A_s - A_b) \times m}{55.84 \times m_o} \quad (2)$$

Where, A_s and A_b are the absorbance of sample and blank, respectively, m is the slope of Fe^{3+} calibration curve with iron concentration varying from 1 to 40 μg (calibration curve: $y = 0.0136x + 0.012$, $R^2=0.996$), 55.84 is the atomic weight of iron, and m_o is mass of sample (g).

2.10.2. Determination of p-Anisidine value

The p-Anisidine value of the extracted oil was determined using an AOCS method (AOCS, 1996) with minor modifications. Briefly, 200 mg of extracted oil was weighed in a test tube and dissolved in 10 mL isooctane. The test tube was vortexed for 30 s and the absorbance of the sample was measured at 350 nm, with isooctane as blank. Subsequently, 5 mL of the experiment solution was mixed with 1 mL of p-Anisidine reagent (0.5 g/200 mL in glacial acetic acid) was added. The mixture was vortexed for 1 min. The sample was placed for 10 min and its absorbance at 350 nm wavelength was measured by microplate reader. The p-Anisidine value was calculated using Eq. (3) and expressed as AU_{350}/g oil.

$$p\text{-Anisidine value} = \frac{10 \times (1.2A_s - A_{S0})}{m} \quad (3)$$

Where, A_s is the absorbance of the sample after reaction with the reagent, A_{S0} is the absorbance of the oil solution with isooctane as solvent, 10 is the volume of isooctane used for sample dissolution, 1.2 is the correction factor for dilution of experiment solution, and m is the mass of oil (g).

2.10.3. Determination of total oxidation value

The total oxidation value (Totox) was used to estimate the oxidation of stabilised oil during storage. It was calculated based on PV and p-Anisidine values using Eq. (4) (Pereira de Abreu et al., 2010).

$$\text{Totox value} = (2 \times \text{peroxide value}) + p\text{-Anisidine value} \quad (4)$$

2.11. Statistical analysis

All measurements were performed in triplicate unless otherwise specified. The experimental data are reported as mean \pm standard deviation. The SPSS statistical software (SPSS 23.0, IBM, Armonk, NY, USA) was used for data analysis. The statistical analysis was carried out using one-way analysis of variance (ANOVA) with Duncan's multiple range test, as a post-hoc test, at a 95% confidence level ($p < 0.05$).

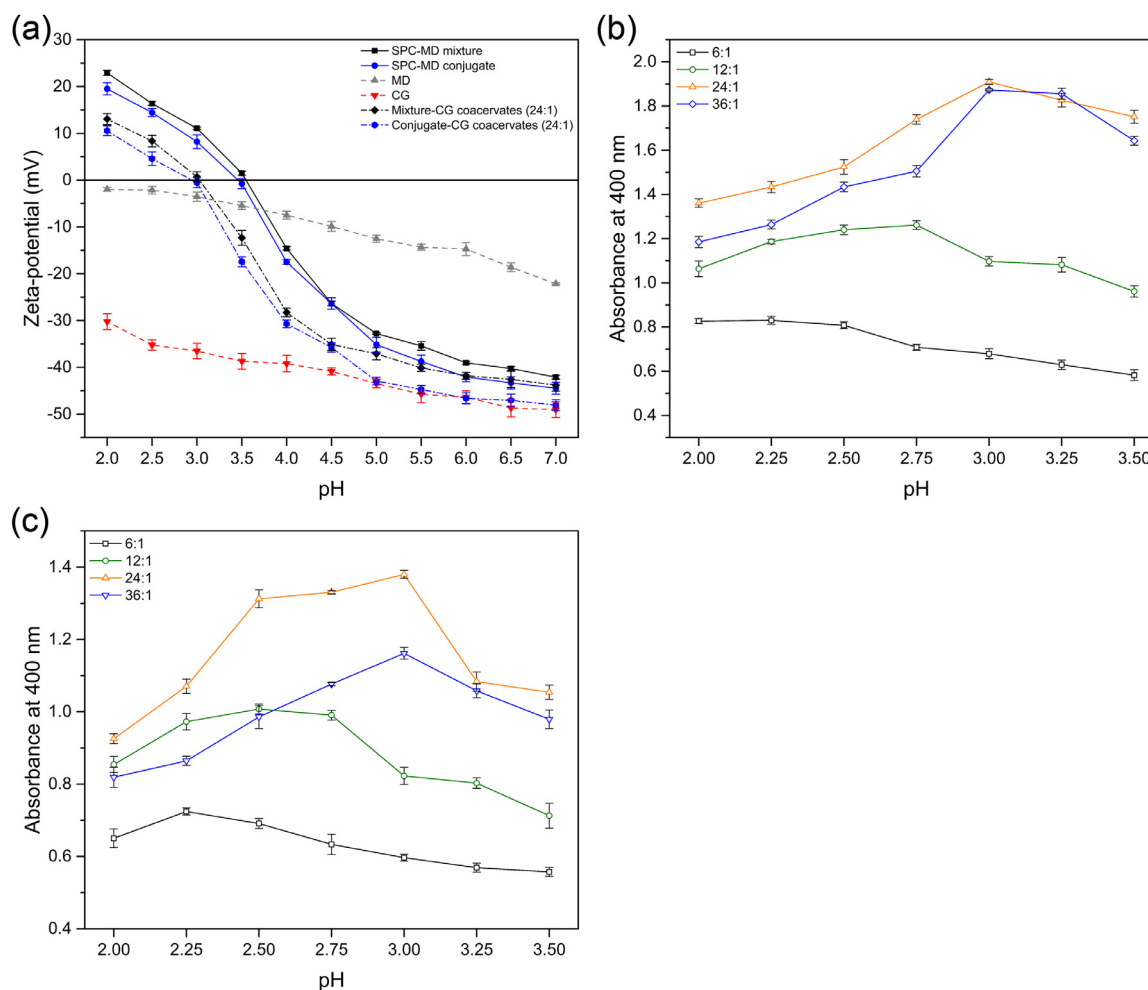


Fig. 2. Optimization of complex coacervation: (a) Zeta-potential of SPC-MD mixture, SPC-MD conjugate, MD, CG, (SPC-MD mixture)-CG coacervates and (SPC-MD conjugate)-CG coacervates at a mixture- or conjugate-to-CG ratio of 24:1 (w/w); Optical density of (SPC-MD mixture)-CG coacervates (b) and (SPC-MD conjugate)-CG coacervates (c) at a mixture- or conjugate-to-CG ratio of 6:1, 12:1, 24:1 and 36:1 (w/w).

3. Results and discussion

3.1. Effect of pH and polymer mixing ratio on SPC-MD-CG complex coacervation

The Zeta-potential values of SPC-MD mixture and conjugate, MD, CG and their complex coacervates are shown in Fig. 2a. All the dispersions showed a decrease of zeta-potential value with the increase of pH. The SPC-MD mixture and SPC-MD conjugate exhibited isoelectric point (pI) around pH 3.6 and 3.5, respectively. The slightly decreased pI value of SPC-MD conjugate was due to the attachment of negatively charged MD (Fig. 2a) on the protein molecular chain during conjugation. CG is an anionic polysaccharide and its zeta-potential value varied from -30.2 to -49.1 mV in the pH range of 2.0–7.0. This result was in line with the surface charge data reported by Bakry et al. (2019). These zeta-potential data indicated that the complex coacervation between the SPC-MD mixture or conjugate and CG would occur when the pH value of the mixture was below 3.5.

The optical density of both (SPC-MD mixture)-CG and (SPC-MD conjugate)-CG solutions at different mixture- and conjugate-to-CG ratios (6:1, 12:1, 24:1 and 36:1, w/w) in the pH range of 2.0–3.5 is shown in Fig. 2b and 2c. The optical density of both systems increased with the increased SPC-MD mixture- or SPC-MD conjugate-to-CG ratio and the maximum optical density was observed at the ratio of 24:1 (w/w) in both cases. The relatively low optical density values of the mixture

at low polymer mixing ratios were mainly due to the steric repulsion caused by excessive CG in the aqueous phase. The unbound polysaccharides are known to inhibit complex coacervation (Duhoranimana et al., 2017). On the other hand, the optical density values decreased when the SPC-MD mixture- or SPC-MD conjugate-to-CG ratio was increased to 36:1 (w/w). This could be attributed to the excessive content of SPC in the system resulting in the interaction between proteins instead of electrostatic interaction with CG. The increase of protein-to-polysaccharide ratio can lead to the increase of protein concentration, which can result in the increased amount of protein-protein aggregation and less interactions between protein and polysaccharides (Aryee and Nickerson, 2012).

The optimum pH for complex coacervation is indicated by the highest optical density value. The optimum pH value increased gradually with the increase of SPC-MD mixture- or SPC-MD conjugate-to-CG ratio. The optimum pH for the complex coacervation between SPC-MD mixture and CG increased from pH 2.25 to 3.25 with the increased mixture-to-CG ratio from 6:1 to 36:1 (w/w) (Fig. 2b). In the complex coacervates produced using high mixture- or conjugate-to-CG ratio, more protein molecules were bound to CG so the system reached its electrical neutrality at a pH value which was closer to the pI of protein. In this study, the highest optical density of (SPC-MD mixture)-CG and (SPC-MD conjugate)-CG systems was found at pH 3.0 with a mixture- or conjugate-to-CG ratio of 24:1 (w/w). This result agreed well with the zeta-potential values of the complex coacervates (Fig. 2a). When the SPC-MD mixture- or SPC-MD conjugate-to-CG ratio was controlled at

24:1 (w/w), the SPC-MD mixture-CG and SPC-MD conjugate-CG systems had pI at approximately pH 3.0 (Fig. 2a). This indicates all the electrostatic charges were neutralised by highest level of electrostatic interactions and insoluble complexes were formed. Thus, the optimum condition for complex coacervation between (SPC-MD) mixture and (SPC-MD) conjugate and CG was mixture- or conjugate-to-CG ratio of 24:1 (w/w) and pH 3.0.

3.2. Rheological properties of coacervates

Rheological properties of the coacervates are important as they suggest the strength of the electrostatic interaction between the participating biopolymers in the system (Schmitt and Turgeon, 2011). The shear viscosity of (SPC-MD mixture)-CG and (SPC-MD conjugate)-CG coacervates formed at different mixing ratios and pH values is shown in Fig. 3a–3d. The viscosity of both complex coacervates showed a decreasing trend with the increase of shear rate within the tested range ($0.1\text{--}120\text{ s}^{-1}$), indicating a typical shear-thinning behavior. A similar trend was also reported in complex coacervates formed between whey protein and gum Arabic (Weinbreck et al., 2004), whey protein and flaxseed gum (Liu et al., 2017) and soy protein and chitosan (Yuan et al., 2017). This shear-thinning behavior of the formed complex coacervates can be attributed to the interruption of hydrogen bonds and other interacting forces between the polymers and water due to application of shear (Zhong et al., 2021).

Both (SPC-MD mixture)-CG and (SPC-MD conjugate)-CG coacervates showed their maximum viscosity at the mixing ratio of 24:1 (w/w) and pH of 3.0 (Fig. 3), indicating the formation of coacervates with the most compact structure corroborating the zeta-potential and optical density (Fig. 2) results. The variation of mixing ratios and pH values of the coacervation process affected the intermolecular electrostatic interactions between protein and polysaccharides, thereby resulting in a loosely packed structure that decreased the overall viscosity of the coacervates compared to the coacervates formed at the optimum conditions (Liu et al., 2017). It can be observed that the (SPC-MD conjugate)-CG coacervate formed at the mixing ratio of 24:1 (w/w) and pH of 3.0 showed the slightly higher viscosity than (SPC-MD mixture)-CG coacervate at a given shear rate. This could be attributed to the more compact structure of SPC-MD conjugate than the SPC-MD mixture, due to the covalent conjugation and which ultimately led to its increased rheological properties (Zhang et al., 2023).

The frequency sweep curves of the coacervates formed at different mixing ratios and pH values within their linear viscoelastic region are shown in Fig. 3e–h. Both (SPC-MD mixture)-CG and (SPC-MD conjugate)-CG coacervates exhibited the increment of storage modulus G' and loss modulus G'' as frequency increased and the G' was always higher than G'' over the tested frequency range, indicating that these coacervates had a dominant elastic behavior (Liu et al., 2017). The maximum G' and G'' values of both complex coacervates were observed at the mixing ratio of 24:1 (w/w) and pH 3.0. It was due to the formation of a highly interconnected gel-like network via the electrostatic interactions between protein and polysaccharides. This result corroborated the observation made in terms of zeta-potential, optical density and shear viscosity of these systems. The conjugate-based coacervates showed slightly higher G' and G'' values than the mixture-based one within the tested frequency range (Fig. 3), due to a more compact structure formed via conjugation. This improved the gel strength and reduced the fluidity of the system and ultimately increased the viscoelasticity. A similar trend was reported in the complexes formed by glycosylated whey protein isolate and chitoooligosaccharide (Yu et al., 2021).

3.3. Physical properties of microcapsules

The characteristics of the spray-dried microcapsules including moisture content, water activity, surface oil content, microencapsulation efficiency and particle size are presented in Table 1. The microcapsules pre-

pared using (SPC-MD mixture)-CG and (SPC-MD conjugate)-CG coacervates as shell material showed moisture contents of 2.7 and 2.8% (w/w), respectively. These values are within safe storage moisture content in commonly produced spray dried food powders and thus conducive for the stability of the core material during storage (Goyal et al., 2015). The water activity of these two microcapsule powders was also around 0.2 which is considered microbiologically stable as spoilage microorganisms are unlikely to grow in this water activity range (Lan et al., 2021).

The encapsulation efficiency of spray-dried microcapsules is shown in Table 1. The surface oil content of microcapsules produced using (SPC-MD conjugate)-CG coacervate as wall material was 1.52% (w/w) which is significantly ($p < 0.05$) lower than the microcapsules by (SPC-MD mixture)-CG coacervate (2.95%, w/w). Hence, the microcapsules produced using (SPC-MD conjugate)-CG coacervate had higher encapsulation efficiency (92.5%). This low surface oil content and high encapsulation efficiency of microcapsules produced using conjugate-based coacervates indicate their ability to protect core material against oxidation more effectively (Yuan et al., 2017). This lower surface oil and higher encapsulation efficiency of microcapsules produced using (SPC-MD conjugate)-CG coacervate could be attributed to the improved solubility and emulsifying properties of SPC after conjugation with MD (Zhang et al., 2023). The improved technofunctional properties of the protein after Maillard reaction made it easier to form a thicker interfacial layers which prevented droplets coalescence during emulsification. The formation of more compact coacervate layers ultimately led to higher encapsulation efficiency (Ifeduba and Akoh, 2016). Muhoza et al. (2022) also reported that the encapsulation efficiency of the core material (cinnamaldehyde) significantly improved when gelatin-low methoxyl pectin conjugate-based coacervates were used at the wall material compared to the one stabilised by the mixture-based coacervates.

3.4. Particle size and morphology of microcapsules

The particle size (D_{50}) of the solid microcapsules is shown in Table 1. The microcapsules produced using SPC-MD mixture-based coacervates were slightly larger than the ones produced using SPC-MD conjugate-based coacervates (8.95 versus 7.66 μm , $p < 0.05$). We reported earlier that the oil-in-water emulsion stabilised using Maillard reaction conjugates as emulsifiers showed smaller particle size and higher stability, compared to the one stabilised by protein itself (Zhang et al., 2023). Agglomeration of particles commonly occurs in the complex coacervation process due to electrostatic complexation between protein and polysaccharides (Muhoza et al., 2022). The improved emulsion stability prevented particle agglomeration due to the enhanced steric repulsion between particles, thereby reducing the particle size of microcapsules (Ifeduba and Akoh, 2015). A similar result was reported in fish oil microcapsulated when soy protein isolate hydrolysate-maltodextrin Maillard reaction products were used as shell material (Zhang et al., 2015).

Fig. 4e and f presents the morphology of the spray-dried microcapsules stabilised by mixture- and conjugate-based coacervates. Both microcapsules exhibited spherical geometry and irregular shape with a wrinkled and uneven surface. This was caused by the uneven shrinkage of particles due to the rapid evaporation of water during spray drying (Chang et al., 2016). Moreover, no noticeable cracks were observed on the surface of the microcapsules and this indicates both coacervates can provide effective protection to the core material against oxygen transfer (Lan et al., 2021). The slightly smaller size of the (SPC-MD conjugate)-CG coated canola oil microcapsules was in agreement with the particle size (D_{50}) results.

3.5. FTIR analysis of spray-dried microcapsules

The FTIR spectra of the wall materials (SPC, SPC-MD conjugate, MD and CG), core material and spray-dried microcapsules are shown in Fig. 4d. In general, SPC showed a typical band at around 1644 cm^{-1}

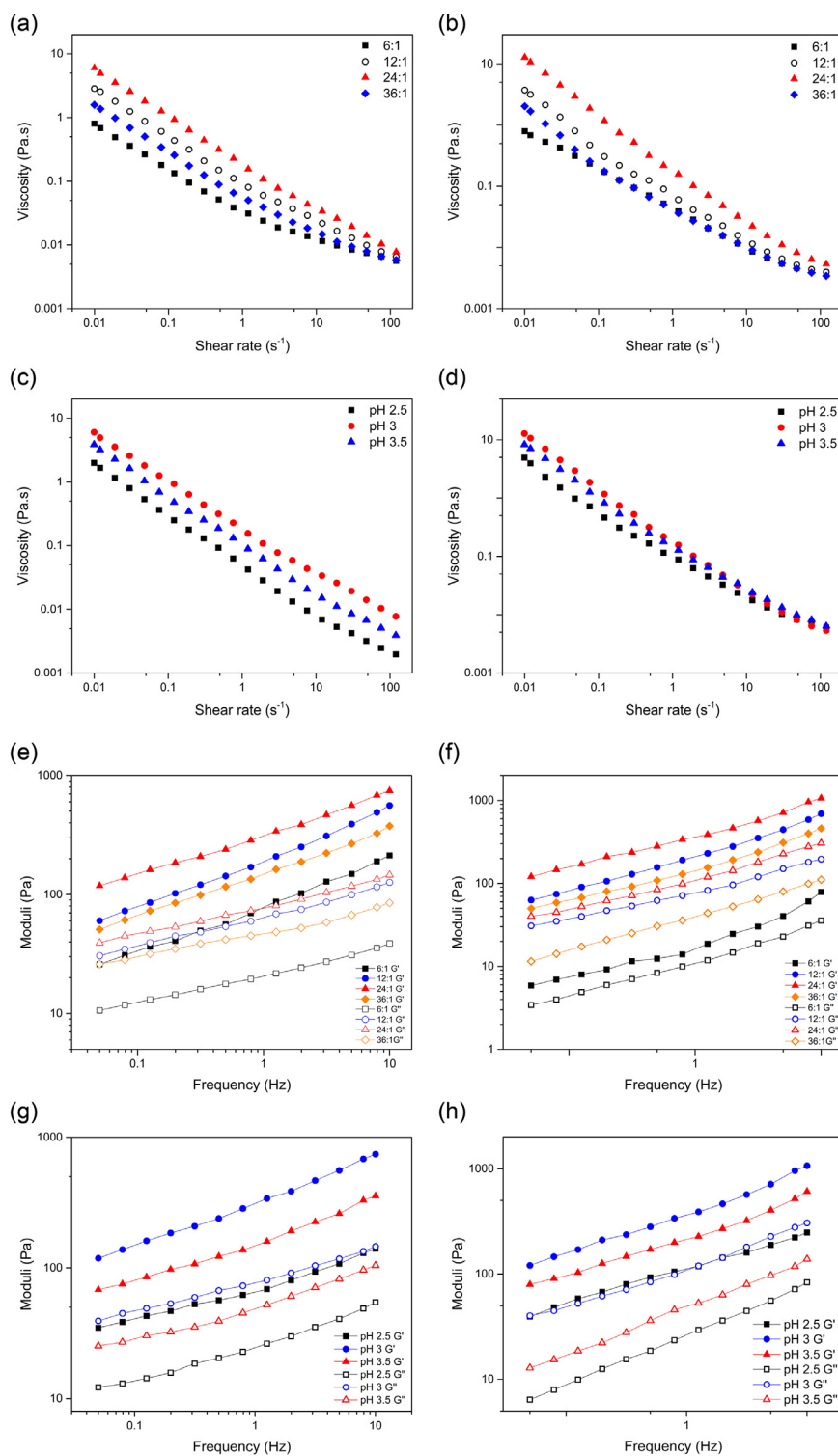


Fig. 3. The viscosities (the former) and viscoelastic modulus (G' and G'') (the latter) of two types of complex coacervates: (a) & (e) (SPC-MD mixture)-CG coacervates as a function of mixing ratio; (b) & (f) (SPC-MD conjugate)-CG coacervates as a function of mixing ratio; (c) & (g) (SPC-MD mixture)-CG coacervates as a function of pH; (d) & (h) (SPC-MD conjugate)-CG coacervates as a function of pH, respectively.

Table 1

Physical properties of the spray dried microcapsules produced using (SPC-MD mixture)-CG and (SPC-MD conjugate)-CG coacervates as wall materials.

Sample	Moisture content (%)	Water activity (a_w)	Surface oil content (%)	Encapsulation efficiency (%)	Particle size D_{50} (μm)
(SPC-MD mixture)-CG canola oil microcapsules	2.68 ± 0.2^a	0.18 ± 0.01^a	2.95 ± 0.14^a	84.5 ± 1.43^a	8.95 ± 0.05^a
(SPC-MD conjugate)-CG canola oil microcapsules	2.83 ± 0.4^a	0.21 ± 0.01^b	1.52 ± 0.2^b	92.5 ± 2.18^b	7.66 ± 0.01^b

Note: The different letters in superscript within a column indicate statistically significant differences ($p < 0.05$) by Duncan's multiple range test.

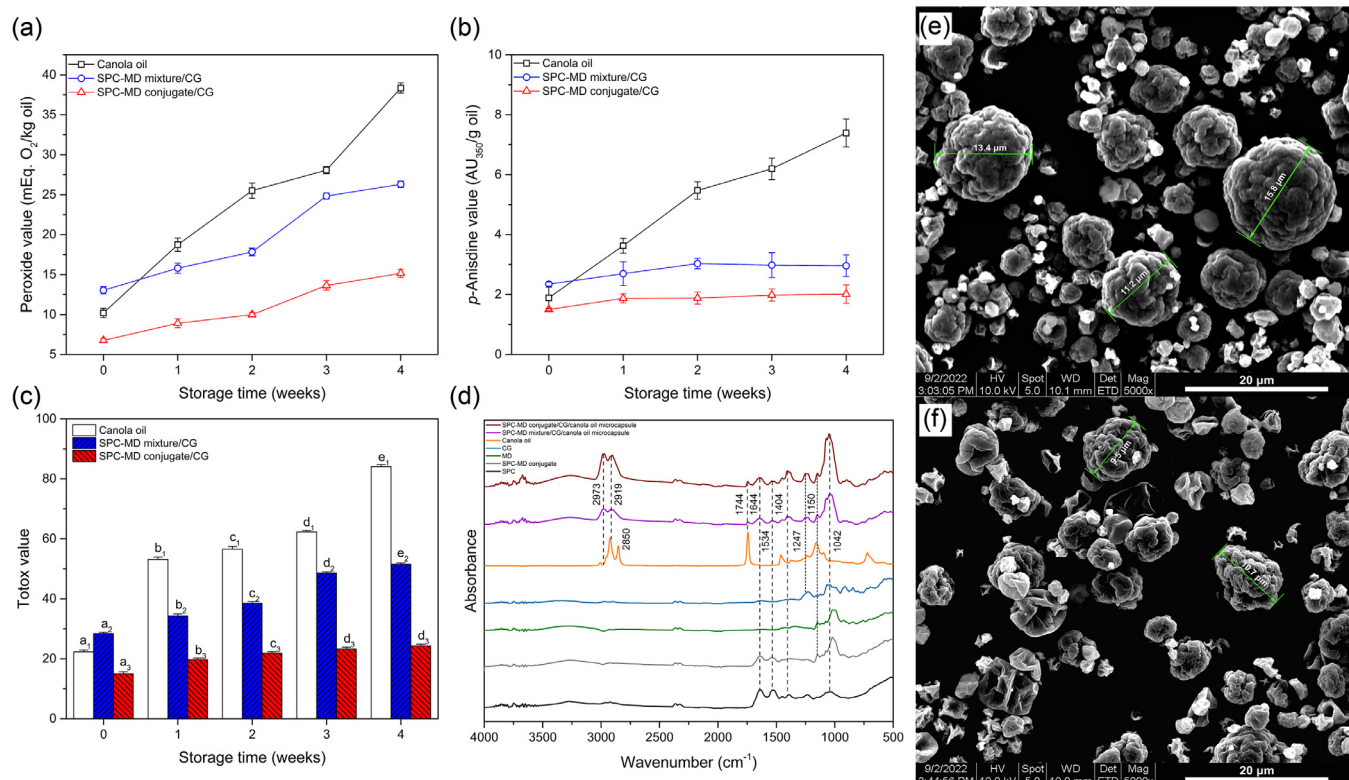


Fig. 4. Oxidative stability of canola oil and microcapsules prepared with different wall materials: (a) peroxide value; (b) *p*-anisidine value and (c) TOTOX values; (d) FTIR spectra of core and wall materials and microcapsules; (e) SEM images of microcapsules stabilised by (SPC-MD mixture)-CG and (f) (SPC-MD conjugate)-CG coacervates.

Note: The different lowercase or uppercase letters above each value indicate significant differences ($p < 0.05$) by Duncan's multiple range test.

of amide I corresponding to C=O stretching, 1534 cm⁻¹ of amide II group from N-H bending and 1404 cm⁻¹ of amide III from C-N stretching (Zhang et al., 2023). In the spectrum of MD, the peaks at around 1150 and 1042 cm⁻¹ were due to the C-C and C-O stretching and the C-H bending, respectively. The spectrum of CG showed a typical band at around 1247 cm⁻¹ due to the asymmetric stretching of S=O. Compared with the spectrum of SPC, the SPC-MD conjugate showed decreased intensities of the amide I, II and III bands, which could be attributed to the consumption of amino acids during the glycation (Wen et al., 2020), indicating the change of secondary structure of SPC after conjugation (Zhang et al., 2023).

The FTIR spectrum of pure canola oil exhibited the typical C-H stretching vibrations of methyl and methylene groups at around 2919 and 2850 cm⁻¹, C=O stretching of ester carbonyl functional groups of the triglycerides at 1744 cm⁻¹ and bending of CH₂ groups at 1150 cm⁻¹ (Ozulku et al., 2017). Both microcapsules exhibited similar band peaks of SPC (amide I, II and III groups), MD and CG (wavenumber at 1247, 1150 and 1042 cm⁻¹) and canola oil (wavenumber 1744 cm⁻¹). The peak at 2919 and 2850 cm⁻¹ of pure canola oil shifted to 2973 and 2919 cm⁻¹ in both microcapsules, respectively, due to interaction between canola oil and the wall materials after the complex coacervation and microencapsulation process (Lan et al., 2021). The observed peaks in the spectra of these microcapsules confirmed the canola oil was successfully encapsulated with (SPC-MD mixture/conjugate)-CG coacervates as wall materials.

3.6. Thermal property of the microcapsules

The thermal characteristics of SPC, SPC-MD conjugates and the oil microcapsules in terms of denaturation temperatures (T_d) and denatu-

ration enthalpy (ΔH) are presented in Table 2. SPC exhibited a T_d value of 66.1 °C, indicating the SPC would denature especially in aqueous medium and when heated for longer time. This result was consistent with Chronakis (2001), who showed that of spirulina protein isolate presented an endothermic peak at 67 °C, and the denaturation of the protein started from 60 °C. Compared to the T_d of SPC, the SPC-MD conjugate showed higher T_d value at 87.8 °C. Moreover, although the enthalpy (ΔH) of SPC-MD conjugate was significantly ($p < 0.05$) lower than SPC (0.18 versus 0.29 W/g), the protein content in conjugate was half that of the native protein. This means that the SPC-MD conjugate can absorb more heat per gram than SPC, indicating the conjugate was more thermally stable than native protein. The increased denaturation temperature and thermal stability of protein in conjugated state were mainly due to the covalent bonding between SPC and MD during Maillard reaction (Liu et al., 2014). On the other hand, the protein in canola oil microcapsule with (SPC-MD mixture)-CG coacervates showed the T_d and ΔH value of 134.7 °C and 16.9 ± 0.02 W/g, respectively. The fact to be aware of is SPC in (SPC-MD mixture)-CG coacervates and (SPC-MD conjugate)-CG coacervates was crosslinked by transglutaminase. Compared to SPC and SPC-MD conjugates, both microcapsules produced by SPC-based coacervates showed increased T_d and ΔH values, which could be due to the crosslinking of SPC molecules by transglutaminase and disuading unfolding and thus resisting denaturation (F. Liu et al., 2016). Moreover, microcapsules with (SPC-MD conjugate)-CG coacervates as the wall material exhibited higher T_d and ΔH values than the one with (SPC-MD mixture)-CG coacervates. This is likely due to the more compact structure of the (SPC-MD conjugate)-CG canola oil coated microcapsules discussed in Section 3.4. It also indicated the improved thermal stability of (SPC-MD conjugate)-CG complex coacervate when used as wall material.

Table 2

Denaturation temperatures (T_d) and degradation enthalpy (ΔH) of SPC, SPC-MD conjugates and the canola oil microcapsules with (SPC-MD mixture)-CG and (SPC-MD conjugate)-CG coacervates as wall material.

Sample	T_d (°C)	ΔH (W/g) (endothermic)
SPC	66.1 ± 0.15 ^d	0.29 ± 0.02 ^c
SPC-MD conjugate	87.8 ± 0.2 ^c	0.18 ± 0.04 ^d
(SPC-MD mixture)-CG canola oil microcapsules	134.7 ± 0.17 ^b	16.9 ± 0.02 ^b
(SPC-MD conjugate)-CG canola oil microcapsules	139.8 ± 0.1 ^a	21.1 ± 0.01 ^a

Note: The different letters in superscript within a column indicate statistically significant differences ($p < 0.05$) by Duncan's multiple range test.

Table 3

Surface elemental compositions of canola oil microcapsules produced using (SPC-MD mixture)-CG and (SPC-MD conjugate)-CG coacervates as wall materials, SPC, SPC-MD conjugate, MD and CG.

	C (wt%)	N (wt%)	O (wt%)	Surface coverage of protein (%) [*]
(SPC-MD mixture)-CG canola oil microcapsules	79.24 ± 0.2 ^a	5.06 ± 0.12 ^d	15.70 ± 0.24 ^f	31.63 ± 0.78 ^d
(SPC-MD conjugate)-CG canola oil microcapsules	72.02 ± 0.13 ^b	8.41 ± 0.16 ^b	20.57 ± 0.1 ^e	52.56 ± 0.94 ^b
SPC	60.33 ± 0.3 ^c	12.11 ± 0.21 ^a	27.56 ± 0.13 ^d	75.69 ± 0.98 ^a
SPC-MD conjugate	60.28 ± 0.13 ^c	7.27 ± 0.14 ^c	32.45 ± 0.21 ^c	45.44 ± 0.64 ^c
Maltodextrin	58.52 ± 0.12 ^d	0	41.48 ± 0.1 ^b	0
Carrageenan	56.09 ± 0.1 ^e	0	43.90 ± 0.1 ^a	0

* Surface coverage of protein was calculated by using a conversion factor of 6.25. Note: The different letters in superscript within a column indicate statistically significant differences ($p < 0.05$) by Duncan's multiple range test.

3.7. Surface composition of the microcapsules

The surface elemental composition of SPC, MD, CG, SPC-MD conjugates, and produced microcapsules are presented in Table 3. SPC had nitrogen and protein contents of 12.1 and 75.7% (w/w), respectively. This result agrees well with the SPC protein content measured by Kjeldahl method. The N and surface protein content of SPC-MD conjugate decreased compared to pure SPC. This was due to the presence of MD, which does not contain N.

As shown in the table, the microcapsule produced using (SPC-MD conjugate)-CG coacervates as the wall material had significantly higher N and protein contents than the one stabilised with the mixture-based coacervates. An increase of surface hydrophobicity and surface-active nature of SPC-MD conjugate was observed after Maillard reaction in our previous study (Zhang et al., 2023). It has been reported that the protein with higher surface-activity tends to accumulate at the air-water interface of the droplets during the spray drying process, which leads to an increase of protein content on the surface of dry powder (Fäldt and Bergenstahl, 1996). Moreover, during the spray drying process, the water present in the droplets diffuses from the interior to the surface. Concurrently, counter diffusion of solutes happens due to concentration gradient of solutes near the air-water interface and the interior of the droplet (Fu et al., 2011). Solutes with smaller molecular weight and lower surface hydrophobicity tend to diffuse more easily towards the interior of the droplet. Since the molecular mass of and size of formed SPC-MD conjugate were higher than the native protein, making it difficult to move to the inner layers, thus resulted in the increase of surface protein content (Fu et al., 2011). The increased surface protein content on the microcapsule also contributed to the decreased surface oil content, discussed in Section 3.3.

A high C content was observed on the microcapsule surface (72–79%) than in wall materials (56–60.3%). This could be due to the presence of free surface oil in the microcapsules (Porrás-Saavedra et al., 2018). The microcapsule produced with (SPC-MD conjugate)-CG coacervates had a lower C content than the one encapsulated with (SPC-MD mixture)-CG coacervates and this result agreed well with the surface oil content data (Section 3.3). When the (SPC-MD mixture)-CG coacervates were used to encapsulate the oil, the resulting microcapsules had significantly lower surface O content than the one stabilised with (SPC-MD conjugate)-CG coacervates (15.70 and 20.57%, respectively). As shown

in the table, MD and CG had O content of 41.48 and 43.90%, respectively. Canola oil is rich in oleic acid (C18:1, C₁₈H₃₄O₂), linoleic acid (C18:2, C₁₈H₃₂O₂) and alpha-linolenic acid (C18:3, C₁₈H₃₀O₂); thus, its theoretical O content is approximately 11% (w/w) (Aldhaidhawi et al., 2017). The low O content on the surface of the microcapsule with (SPC-MD mixture)-CG coacervates as shell material was contributed by its high surface oil content.

3.8. Oxidative stability of the microcapsules

The oxidative stability of microencapsulated canola oil stored at 40 °C for 4 weeks in terms of PV, *p*-AV and TOTOX values is shown in Fig. 4a–4c. These values of the unencapsulated and encapsulated oil microcapsules increased gradually during storage, however, the most rapid oxidation was observed in the unencapsulated canola oil. This indicates the sound protective effect of both (SPC-MD mixture)-CG coacervate and (SPC-MD conjugate)-CG coacervate. The canola oil microcapsules produced using (SPC-MD conjugate)-CG coacervate always exhibited lower PV, *p*-AV and TOTOX values than the one encapsulated in (SPC-MD mixture)-CG coacervates. This could be attributed to the low surface oil content of the microcapsules produced using conjugate-based coacervates (Section 3.3) and also the improved antioxidant capacity of SPC after Maillard reaction. Moreover, the conjugate-based coacervates formed more compact capsule wall which offered more effective physical barrier to encapsulated canola oil against oxygen (Ifeduba and Akoh, 2016). A similar result was observed in the stearidonic acid soybean oil encapsulated by gelatin-gum Arabic conjugate (Ifeduba and Akoh, 2016). The *p*-AV and TOTOX values of canola oil microcapsules encapsulated in (SPC-MD conjugate)-CG coacervate remained almost unchanged during the last 2 weeks of storage. This indicated that the secondary oxidation was effectively inhibited; thus, the Maillard reaction induced (SPC-MD conjugate)-CG coacervates can be considered as a promising wall material for encapsulating oxygen-sensitive oils.

4. Conclusion

Spirulina protein concentrate (SPC)- maltodextrin (MD) conjugates formed by Maillard reaction via the wet-heating route and complex coacervates of these conjugates with carrageenan (CG) were successfully developed. Microcapsules of oxidation sensitive canola oil were

produced using these (SPC-MD conjugate)-CG coacervates. The complex coacervation process was optimised at SPC-MD conjugate to CG ratio of 24:1 (w/w) at pH 3.0. The microcapsules produced using (SPC-MD conjugate)-CG coacervates had lower surface oil content, higher encapsulation efficiency compared to those produced using (SPC-MD mixture)-CG coacervates. The denaturation temperature of SPC in (SPC-MD conjugate)-CG canola oil microcapsules was much higher compared to unconjugated SPC. Higher protein and lower surface oil contents were observed on the microcapsule surface when produced using conjugate-based coacervates as wall material and provided improved stability against oxidation. This study shows that complex coacervates of priori conjugated protein-polysaccharide systems are better encapsulating shell materials than simple protein-polysaccharide complex coacervated. This study also shows that, the novel spirulina protein can be confidently used as encapsulating shell material after conjugating with polysaccharide followed by complex coacervation. The outcome will be of practical importance to the food industry.

Ethical statement

Hereby, I (Zijia Zhang) consciously assure that for the manuscript "Improving functional properties of Spirulina protein by covalent conjugation followed by complex coacervation processes" the following is fulfilled:

This research does not involve the use of animal and human subjects.

Declaration of Competing Interest

The authors declare that they have no known competing financial interests or personal relationships that could have appeared to influence the work reported in this paper.

CRediT authorship contribution statement

Zijia Zhang: Conceptualization, Methodology, Writing – original draft. **Bo Wang:** Conceptualization, Supervision, Writing – review & editing. **Greg Holden:** Conceptualization, Supervision. **Jie Chen:** Conceptualization, Supervision. **Benu Adhikari:** Conceptualization, Supervision, Writing – review & editing.

Data availability

Data will be made available on request.

References

- Aldhaidhawi, M., Chiriac, R., Badescu, V., 2017. Ignition delay, combustion and emission characteristics of Diesel engine fueled with rapeseed biodiesel – A literature review. *Renew. Sustain. Energy Rev.* 73, 178–186. doi:10.1016/j.rser.2017.01.129.
- Gunstone, F.A.O.C.S., 1996. *Official methods and recommended practices of the American oil chemists' society method Cd 18-90. P-Anisidine Value*, 4th ed. AOCS Press, Champaign, IL.
- Aryee, F.N.A., Nickerson, M.T., 2012. Formation of electrostatic complexes involving mixtures of lentil protein isolates and gum Arabic polysaccharides. *Food Res. Int.* 48 (2), 520–527. doi:10.1016/j.foodres.2012.05.012.
- Bakry, A.M., Huang, J., Zhai, Y., Huang, Q., 2019. Myofibrillar protein with κ - or λ -carrageenans as novel shell materials for microencapsulation of tuna oil through complex coacervation. *Food Hydrocoll.* 96, 43–53. doi:10.1016/j.foodhyd.2019.04.070.
- Chang, C., Varankovich, N., Nickerson, M.T., 2016. Microencapsulation of canola oil by lentil protein isolate-based wall materials. *Food Chem.* 212, 264–273. doi:10.1016/j.foodchem.2016.05.136.
- Chronakis, I.S., 2001. Gelation of Edible Blue-Green Algae Protein Isolate (*Spirulina platensis* Strain Pacifica): thermal Transitions, Rheological Properties, and Molecular Forces Involved. *J. Agric. Food Chem.* 49 (2), 888–898. doi:10.1021/jf0005059.
- Dorđević, V., Balanč, B., Belščak-Cvitanović, A., Lević, S., Trifković, K., Kalušević, A., Nedović, V., 2015. Trends in encapsulation technologies for delivery of food bioactive compounds. *Food Eng. Rev.* 7 (4), 452–490. doi:10.1007/s12393-014-9106-7.
- Duhoanimana, E., Karangwa, E., Lai, L., Xu, X., Yu, J., Xia, S., Habinshuti, I., 2017. Effect of sodium carboxymethyl cellulose on complex coacervates formation with gelatin: coacervates characterization, stabilization and formation mechanism. *Food Hydrocoll.* 69, 111–120. doi:10.1016/j.foodhyd.2017.01.035.
- Eltweri, A.M., Thomas, A.L., Metcalfe, M., Calder, P.C., Dennison, A.R., Bowrey, D.J., 2017. Potential applications of fish oils rich in omega-3 polyunsaturated fatty acids in the management of gastrointestinal cancer. *Clin. Nutr.* 36 (1), 65–78. doi:10.1016/j.clnu.2016.01.007.

- Fäldt, P., Bergenståhl, B., 1996. Spray-dried whey protein/lactose/soybean oil emulsions. 1. Surface composition and particle structure. *Food Hydrocoll.* 10 (4), 421–429. doi:10.1016/S0268-005X(96)80020-8.
- Fu, N., Woo, M.W., Chen, X.D., 2011. Colloidal transport phenomena of milk components during convective droplet drying. *Colloids Surf. B* 87 (2), 255–266. doi:10.1016/j.colsurfb.2011.05.026.
- Gaiani, C., Morand, M., Sanchez, C., Tehrani, E.A., Jacquot, M., Schuck, P., Scher, J., 2010. How surface composition of high milk proteins powders is influenced by spray-drying temperature. *Colloids Surf. B* 75 (1), 377–384. doi:10.1016/j.colsurfb.2009.09.016.
- Ganesan, K., Sukalingam, K., Xu, B., 2018. Impact of consumption and cooking manners of vegetable oils on cardiovascular diseases- a critical review. *Trends Food Sci. Technol.* 71, 132–154. doi:10.1016/j.tifs.2017.11.003.
- Goyal, A., Sharma, V., Sihag, M.K., Tomar, S.K., Arora, S., Sabikhi, L., Singh, A.K., 2015. Development and physico-chemical characterization of microencapsulated flaxseed oil powder: a functional ingredient for omega-3 fortification. *Powder Technol.* 286, 527–537. doi:10.1016/j.powtec.2015.08.050.
- Ifeduba, E.A., Akoh, C.C., 2015. Microencapsulation of stearidonic acid soybean oil in complex coacervates modified for enhanced stability. *Food Hydrocoll.* 51, 136–145. doi:10.1016/j.foodhyd.2015.05.008.
- Ifeduba, E.A., Akoh, C.C., 2016. Microencapsulation of stearidonic acid soybean oil in Maillard reaction-modified complex coacervates. *Food Chem.* 199, 524–532. doi:10.1016/j.foodchem.2015.12.011.
- Kim, E.H., Chen, X.D., Pearce, D., 2005. Melting characteristics of fat present on the surface of industrial spray-dried dairy powders. *Colloids Surf. B* 42 (1), 1–8. doi:10.1016/j.colsurfb.2005.01.004.
- Kaushik, P., Dowling, K., Barrow, C.J., Adhikari, B., 2015. Microencapsulation of omega-3 fatty acids: a review of microencapsulation and characterization methods. *J. Funct. Foods* 19, 868–881. doi:10.1016/j.jff.2014.06.029.
- Lan, Y., Ohm, J.B., Chen, B., Rao, J., 2021. Microencapsulation of hemp seed oil by pea protein isolate–sugar beet pectin complex coacervation: influence of coacervation pH and wall/core ratio. *Food Hydrocoll.* 113, 106423. doi:10.1016/j.foodhyd.2020.106423.
- Liu, F., Majeed, H., Antoniou, J., Li, Y., Ma, Y., Yokoyama, W., Zhong, F., 2016. Tailoring physical properties of transglutaminase-modified gelatin films by varying drying temperature. *Food Hydrocoll.* 58, 20–28. doi:10.1016/j.foodhyd.2016.01.026.
- Liu, J., Shim, Y.Y., Shen, J., Wang, Y., Reaney, M.J.T., 2017. Whey protein isolate and flaxseed (*Linum usitatissimum* L.) gum electrostatic coacervates: turbidity and rheology. *Food Hydrocoll.* 64, 18–27. doi:10.1016/j.foodhyd.2016.10.006.
- Liu, Q., Kong, B., Han, J., Sun, C., Li, P., 2014. Structure and antioxidant activity of whey protein isolate conjugated with glucose via the Maillard reaction under dry-heating conditions. *Food Structure* 1 (2), 145–154. doi:10.1016/j.foosr.2013.11.004.
- Martinez-Alvarenga, M.S., Martinez-Rodriguez, E.Y., Garcia-Amezquita, L.E., Olivas, G.I., Zamudio-Flores, P.B., Acosta-Muniz, C.H., Sepulveda, D.R., 2014. Effect of Maillard reaction conditions on the degree of glycation and functional properties of whey protein isolate – Maltodextrin conjugates. *Food Hydrocoll.* 38, 110–118. doi:10.1016/j.foodhyd.2013.11.006.
- Muhoza, B., Harindintwali, J.D., Qi, B., Zhang, S., Li, Y., 2022. Conjugation Induced by wet-heating of gelatin and low methoxyl pectin improves the properties and stability of microcapsules prepared by complex coacervation. *Food Biophys.* doi:10.1007/s11483-022-09754-7.
- Onwezen, M.C., Bouwman, E.P., Reinders, M.J., Dagevos, H., 2021. A systematic review on consumer acceptance of alternative proteins: pulses, algae, insects, plant-based meat alternatives, and cultured meat. *Appetite* 159, 105058. doi:10.1016/j.appet.2020.105058.
- Oppedisano, F., Macri, R., Gliozzi, M., Musolino, V., Carresi, C., Maiuolo, J., Mollace, V., 2020. The anti-inflammatory and antioxidant properties of n-3 PUFAs: their role in cardiovascular protection. *Biomedicines* 8 (9), 306. doi:10.3390/biomedicines8090306.
- Ozulku, G., Yildirim, R.M., Toker, O.S., Karasu, S., Durak, M.Z., 2017. Rapid detection of adulteration of cold pressed sesame oil adulterated with hazelnut, canola, and sunflower oils using ATR-FTIR spectroscopy combined with chemometric. *Food Control.* 82, 212–216. doi:10.1016/j.foodcont.2017.06.034.
- Pereira de Abreu, D.A., Losada, P.P., Maroto, J., Cruz, J.M., 2010. Evaluation of the effectiveness of a new active packaging film containing natural antioxidants (from barley husks) that retard lipid damage in frozen Atlantic salmon (*Salmo salar* L.). *Food Res. Int.* 43 (5), 1277–1282. doi:10.1016/j.foodres.2010.03.019.
- Pham, L.B., Wang, B., Zisu, B., Truong, T., Adhikari, B., 2020. Microencapsulation of flaxseed oil using polyphenol-adsorbed flaxseed protein isolate-flaxseed gum complex coacervates. *Food Hydrocoll.* 107, 105944. doi:10.1016/j.foodhyd.2020.105944.
- Porrás-Saavedra, J., Alamilla-Beltrán, L., Lartundo-Rojas, L., de Jesús Perea-Flores, Ma., Yáñez-Fernández, J., Palacios-González, E., Gutiérrez-López, G. F., 2018. Chemical components distribution and morphology of microcapsules of paprika oleoresin by microscopy and spectroscopy. *Food Hydrocoll.* 81, 6–14. doi:10.1016/j.foodhyd.2018.02.005.
- Rawiwan, P., Peng, Y., Paramayuda, I.G.P.B., Quek, S.Y., 2022. Red seaweed: a promising alternative protein source for global food sustainability. *Trends Food Sci. Technol.* 123, 37–56. doi:10.1016/j.tifs.2022.03.003.
- Ray, S., Raychaudhuri, U., Chakraborty, R., 2016. An overview of encapsulation of active compounds used in food products by drying technology. *Food Biosci.* 13, 76–83. doi:10.1016/j.fbio.2015.12.009.
- Rudke, A.R., Heleno, S.A., Fernandes, I.P., Prieto, M.A., Gonçalves, O.H., Rodrigues, A.E., Barreiro, M.F., 2019. Microencapsulation of ergosterol and *Agaricus bisporus* L. extracts by complex coacervation using whey protein and chitosan: optimization study using response surface methodology. *LWT* 103, 228–237. doi:10.1016/j.lwt.2019.01.018.

- Schmitt, C., Turgeon, S.L., 2011. Protein/polysaccharide complexes and coacervates in food systems. *Adv. Colloid Interface Sci.* 167 (1), 63–70. doi:[10.1016/j.cis.2010.10.001](https://doi.org/10.1016/j.cis.2010.10.001).
- Shantha, N.C., Decker, E.A., 1994. Rapid, sensitive, iron-based spectrophotometric methods for determination of peroxide values of food lipids. *J. AOAC Int.* 77 (2), 421–424. doi:[10.1093/jaoac/77.2.421](https://doi.org/10.1093/jaoac/77.2.421).
- Wang, B., Adhikari, B., Barrow, C.J., 2014. Optimisation of the microencapsulation of tuna oil in gelatin–sodium hexametaphosphate using complex coacervation. *Food Chem.* 158, 358–365. doi:[10.1016/j.foodchem.2014.02.135](https://doi.org/10.1016/j.foodchem.2014.02.135).
- Weinbreck, F., Wientjes, R.H.W., Nieuwenhuijse, H., Robijn, G.W., de Kruif, C.G., 2004. Rheological properties of whey protein/gum arabic coacervates. *J. Rheol. N Y* 48 (6), 1215–1228. doi:[10.1122/1.1795191](https://doi.org/10.1122/1.1795191), N Y.
- Wen, C., Zhang, J., Qin, W., Gu, J., Zhang, H., Duan, Y., Ma, H., 2020. Structure and functional properties of soy protein isolate-lentinan conjugates obtained in Maillard reaction by slit divergent ultrasonic assisted wet heating and the stability of oil-in-water emulsions. *Food Chem.* 331, 127374. doi:[10.1016/j.foodchem.2020.127374](https://doi.org/10.1016/j.foodchem.2020.127374).
- Yu, J., Wang, Q., Zhang, H., Qin, X., Chen, H., Corke, H., Liu, G., 2021. Increased stability of curcumin-loaded pickering emulsions based on glycated proteins and chitoooligosaccharides for functional food application. *LWT* 148, 111742. doi:[10.1016/j.lwt.2021.111742](https://doi.org/10.1016/j.lwt.2021.111742).
- Yuan, Y., Kong, Z.Y., Sun, Y.E., Zeng, Q.Z., Yang, X.Q., 2017. Complex coacervation of soy protein with chitosan: constructing antioxidant microcapsule for algal oil delivery. *LWT* 75, 171–179. doi:[10.1016/j.lwt.2016.08.045](https://doi.org/10.1016/j.lwt.2016.08.045).
- Zhang, Y., Tan, C., Abbas, S., Eric, K., Xia, S., Zhang, X., 2015. Modified SPI improves the emulsion properties and oxidative stability of fish oil microcapsules. *Food Hydrocoll.* 51, 108–117. doi:[10.1016/j.foodhyd.2015.05.001](https://doi.org/10.1016/j.foodhyd.2015.05.001).
- Zhang, Z., Holden, G., Wang, B., Adhikari, B., 2023. Maillard reaction-based conjugation of Spirulina protein with maltodextrin using wet-heating route and characterisation of conjugates. *Food Chem.* 406, 134931. doi:[10.1016/j.foodchem.2022.134931](https://doi.org/10.1016/j.foodchem.2022.134931).
- Zheng, J.X., Yin, H., Shen, C.C., Zhang, L., Ren, D.F., Lu, J., 2020. Functional and structural properties of spirulina phycocyanin modified by ultra-high-pressure composite glycation. *Food Chem.* 306, 125615. doi:[10.1016/j.foodchem.2019.125615](https://doi.org/10.1016/j.foodchem.2019.125615).
- Zhong, W., Li, C., Diao, M., Yan, M., Wang, C., Zhang, T., 2021. Characterization of interactions between whey protein isolate and hyaluronic acid in aqueous solution: effects of pH and mixing ratio. *Colloids Surf. B* 203, 111758. doi:[10.1016/j.colsurfb.2021.111758](https://doi.org/10.1016/j.colsurfb.2021.111758).